

Carbon paste electrode modified with Fe₃O₄ nanoparticles and BMI.PF₆ ionic liquid for determination of estrone by square-wave voltammetry

Fernanda Moreira¹ · Tatiane de Andrade Maranhão¹ · Almir Spinelli¹

Received: 18 May 2017 / Revised: 13 June 2017 / Accepted: 14 June 2017 / Published online: 27 June 2017
© Springer-Verlag GmbH Germany 2017

Abstract A carbon paste electrode (CPE) modified with Fe₃O₄ nanoparticles (Fe₃O₄ NP) and the ionic liquid 1-butyl-3-methylimidazolium hexafluorophosphate (IL BMI.PF₆) was employed for the electroanalytical determination of estrone (E1) by square-wave voltammetry (SWV). At the modified electrode, cyclic voltammograms of E1 in B–R buffer (pH 12.0) showed an adsorption-controlled irreversible oxidation peak at around +0.365 V. The anodic current increased by a factor of five times and the peak potential shifted 65 mV to less positive values compared with the unmodified CPE. Under optimized conditions, the calibration curve obtained showed two linear ranges: from 4.0 to 9.0 μmol L⁻¹ and from 9.0 to 100.0 μmol L⁻¹. The limits of detection (LOD) and quantification (LOQ) attained were 0.47 and 4.0 μmol L⁻¹, respectively. The proposed modified electrode was applied to the determination of E1 in pork meat samples. Data provided by the proposed modified electrode were compared with data obtained by UV–vis spectroscopy. The outstanding performance of the electrochemical device indicates that Fe₃O₄ NP and the IL BMI.PF₆ are promising materials for the preparation of chemically modified electrodes for the determination of E1.

Keywords Carbon paste electrode · Fe₃O₄ nanoparticles · Ionic liquid · Estrone · Pork meat · Square-wave voltammetry

Introduction

Chemically modified electrodes (CMEs) have attracted great attention in the past decades because they improve the sensitivity and selectivity of electroanalytical methods. Various materials have been proposed for the modification of electrodes including graphene [1], carbon nanotubes [2], ionic liquids (ILs) [3, 4], and nanoparticles of iron (Fe NP) [5], iron (III) oxide (Fe₂O₃ NP) [6, 7], and iron (II, III) oxide (Fe₃O₄ NP) [8–12]. In recent years, modified carbon paste electrodes (CPEs) have become an attracting material for the electrochemical detection of various analytes due to their low cost, ease of preparation, renewable surface, and the stability of the electrochemical response [2, 8, 13–15]. Moreover, the feasibility of incorporating different modifiers during the paste preparation permits the fabrication of electrodes with the desired composition and predetermined properties.

Magnetic nanoparticles of iron (II, III) oxide (Fe₃O₄ NP) have been used for the modification of electrodes due to their characteristics such as large surface area, good biocompatibility, strong superparamagnetism, low toxicity, and ease of preparation [16–18]. As examples, carbon paste electrodes modified with Fe₃O₄ have been used for the determination of warfarin in blood serum and urine samples [8], ascorbic and folic acids in herbal life multivitamin [13], and estrin in pharmaceutical and urine samples [11].

Another class of compounds that has attracted the attention of researchers as modifiers of electrodes is ILs [4, 15, 19, 20]. Many interesting properties can be obtained from these materials such as good chemical and thermal stability, wide electrochemical potential window, high ionic conductivity, and catalytic activity

Electronic supplementary material The online version of this article (doi:10.1007/s10008-017-3678-0) contains supplementary material, which is available to authorized users.

✉ Almir Spinelli
almir.spinelli@ufsc.br

¹ Grupo de Estudos de Processos Eletroquímicos e Eletroanalíticos, Departamento de Química, Centro de Ciências Físicas e Matemáticas—CFM, Universidade Federal de Santa Catarina—UFSC, Campus Universitário Reitor João David Ferreira Lima, Florianópolis, SC 88040-900, Brazil

[1, 3, 15, 20–23]. These properties make ILs interesting materials for modification of electrodes, particularly CPEs. Several studies have provided information on the preparation of CPEs using ILs as the binder (total or partial) to replace the non-conductive mineral oil [4, 15, 19]. This simple modification normally improves the reversibility of electrochemical reactions, increases the electron transfer rate, and decreases the overpotential of the reactions of some organic compounds [1, 3, 4, 15]. The use of ILs together with nanomaterials such as metallic nanoparticles is a promising combination for the development of more selective and sensitive analytical devices [9, 21].

Endocrine disruptors (EDCs) are considered as one of the major classes of environmental contaminants that can interfere with the operation of the endocrine system leading to alterations in the growth, development, and reproduction of animals and humans [24, 25]. Among the EDCs, estrogens cause greater concern, both for their ability to cause endocrine disruption and for the amount that is introduced into the environment [26, 27]. Estrone (E1) (Fig. 1), estradiol (E2), and estriol (E3), the three major estrogens found in females, are among the naturally occurring EDCs.

E1 is one of the estrogens produced and then excreted by humans and other animals. Consequently, it can enter the environment through the discharge of domestic sewage effluents and disposal of animal waste, since it is not efficiently removed by traditional methods of water treatment [24, 28, 29]. Moreover, E1 may be present as a residue in meat, since it is one of the metabolites of estradiol, a hormone that can be illegally applied in the breeding of animals and therefore consumed in foods [30–32]. In consideration of the possible harmful effects on public health, the use of natural or artificial substances for growth or fattening of slaughter animals has been prohibited in Brazil, with permission only for therapeutic purposes [33]. Therefore, it is of great importance to develop fast and efficient electrochemical devices for proper control of this estrogen.

The determination of E1 has been well reported in literature and several procedures including chromatographic techniques [29, 34–36], electrophoresis [28, 37], and electrochemical methods [1, 24, 38] are described. Due to its operational simplicity, low cost, fast response, high sensitivity, and the possibility of miniaturization and automation of equipment, interest in electro-analytical methodologies has been growing, especially the use of modified electrodes. A few authors have reported the

combination of Fe_3O_4 NP and ILs to prepare modified electrodes [9, 39]. However, the application of CPEs modified with Fe_3O_4 NP and the IL BMI.PF₆ for the detection of E1 in pork meat, at our acknowledgement, has not yet been reported.

In this context, the aim of this research work was to prepare a CPE modified with Fe_3O_4 NP and the IL BMI.PF₆ and to test it for the determination of the E1 in pork meat samples using the square-wave voltammetry (SWV) technique.

Experimental

Reagents and solutions

All chemicals were of analytical grade. They were purchased from Sigma-Aldrich and used without further purification. Graphite powder (GP), mineral oil (MO), and Fe_3O_4 NP were used to build the unmodified and modified CPEs. According to the manufacturer, the size of Fe_3O_4 NP is <50 nm. The aqueous solutions were prepared with water purified using a Milli-Q system (Millipore, USA) with a resistivity of 18.2 M Ω cm. A stock solution of 4 mmol L⁻¹ E1 in ethanol was prepared daily and less concentrated solutions were prepared by dilution. The supporting electrolytes Britton–Robinson (B–R) and Ringer's buffers and NaOH solutions were used for the electrochemical experiments. They were prepared in the concentration of 0.2 mol L⁻¹ and their pH was then adjusted to the desired level with 1.0 mol L⁻¹ HCl or NaOH. Solutions of KCl and K₃[Fe(CN)₆] were used to electrochemically characterize the modified CPEs.

Preparation of CPE/ Fe_3O_4 NP-BMI.PF₆

The CPE/ Fe_3O_4 NP-BMI.PF₆ was prepared according to the optimized conditions in a 3² factorial design (Table S1 and Fig. S1). A paste with mass of 200 mg was prepared using 140 mg (70% *m/m*) of GP + Fe_3O_4 NP and 60 mg (30% *m/m*) of MO + IL BMI.PF₆. A mass of 133 mg GP was macerated manually with 7 mg Fe_3O_4 NP for 10 min to obtain a uniform dispersion of the Fe_3O_4 NP in the GP. Next, 45 mg of MO was added and macerated for 10 min, followed by the addition of the 15 mg of IL BMI.PF₆ and maceration again for 10 min, to obtain the modified paste. The modified paste was introduced into a plastic syringe with a volume of 1.0 mL and a copper wire was inserted to obtain the electrical contact. The CPE/ Fe_3O_4 NP-BMI.PF₆ were allowed to dry at room temperature for 7 days. After use and when necessary, a new surface was obtained by pushing an excess of the paste out of the syringe tube and scraping on a weighing paper. For comparison purposes, electrodes with different composition were prepared only with Fe_3O_4 NP (CPE/ Fe_3O_4 NP) and IL BMI.PF₆ (CPE/BMI.PF₆), as well as an unmodified CPE.

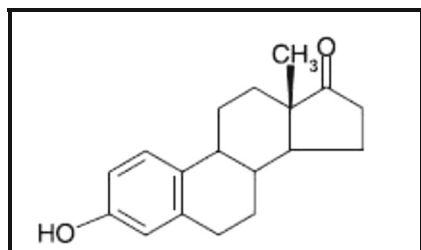


Fig. 1 Chemical structure of estrone

Morphological characterization

The electrodes with and without modifications were characterized by field emission gun scanning electron microscopy (FEG-SEM) using a JEM-2100 (JEOL, Japan). Samples of unmodified and modified carbon paste were placed on the surface of a stub with an area of 1.5 cm² containing silver glue as an adhesive. After drying for 10 min, the excess material was removed. The samples were stored in a vacuum desiccator at room temperature (25 ± 2 °C) for 24 h.

Electrochemical experiments

The voltammetric experiments using cyclic (CV) and square-wave voltammetry (SWV) were carried out at room temperature (25 ± 2 °C) with a potentiostat, model EmStat2 (Palm Instruments BV, The Netherlands), coupled to a personal computer with the PStTrace software package (version 4.7) for the acquisition and processing of data. The electrochemical system was composed of an electrochemical cell with a capacity of 15 mL containing three electrodes: a modified or unmodified CPE as the working electrode, an Ag/AgCl reference electrode (3.0 mol L⁻¹ KCl), and a platinum plate as the auxiliary electrode. For the construction of the calibration curve, the SWV measurements were performed sweeping the potential from +0.1 to +0.6 V at scan increment (ΔE_s) of 2.8 mV, amplitude (a) of 90 mV, and frequency (f) of 30 Hz, after successive additions of a stock solution of E1. After each addition, the solution was stirred in order to homogenize its composition. The electrochemical impedance spectroscopy (EIS) was performed using a PalmSens³ potentiostat (PalmSens BV, The Netherlands). The EIS spectra were obtained in 0.5 mol L⁻¹ KCl containing 5.0 mmol L⁻¹ K₃[Fe(CN)₆]/K₄[Fe(CN)₆] (1:1), using the open circuit potential mode, amplitude of 5 mV, and a frequency range of 0.1 to 50,000 Hz.

Samples preparation

Pork meat acquired at a local store was used to prepare the samples. The meat was crushed in a meat grinder and stored at 4 °C until analysis. For the preparation of the samples, the procedure described by Wang and coworkers [32] was adapted. Samples (around 50 g) of the crushed meat were fortified with standard solutions of E1: sample A (70.0 μmol L⁻¹), B (80.0 μmol L⁻¹), and C (90.0 μmol L⁻¹). In the next step, 50 mL of ethanol was added to the spiked crushed meat followed by sonication for 20 min at room temperature in a closed recipient. The organic phase (around 20 mL) was diluted to 25 mL with ethanol and used as the pork meat sample. The electroanalytical determinations were repeated eight times applying the external calibration method. Prior to the experiment, the standard addition method was carried out to identify any matrix effect.

Comparative spectroscopic method

The UV–vis spectroscopy was used as comparative technique. The analysis was carried out in the wavelength range of 200 to 800 nm using a Shimadzu UV-1800 spectrophotometer (Japan). A quartz cell with an optical path of 1.0 cm was used. The absorbance of the solutions containing different concentrations of E1 was determined at 282 nm.

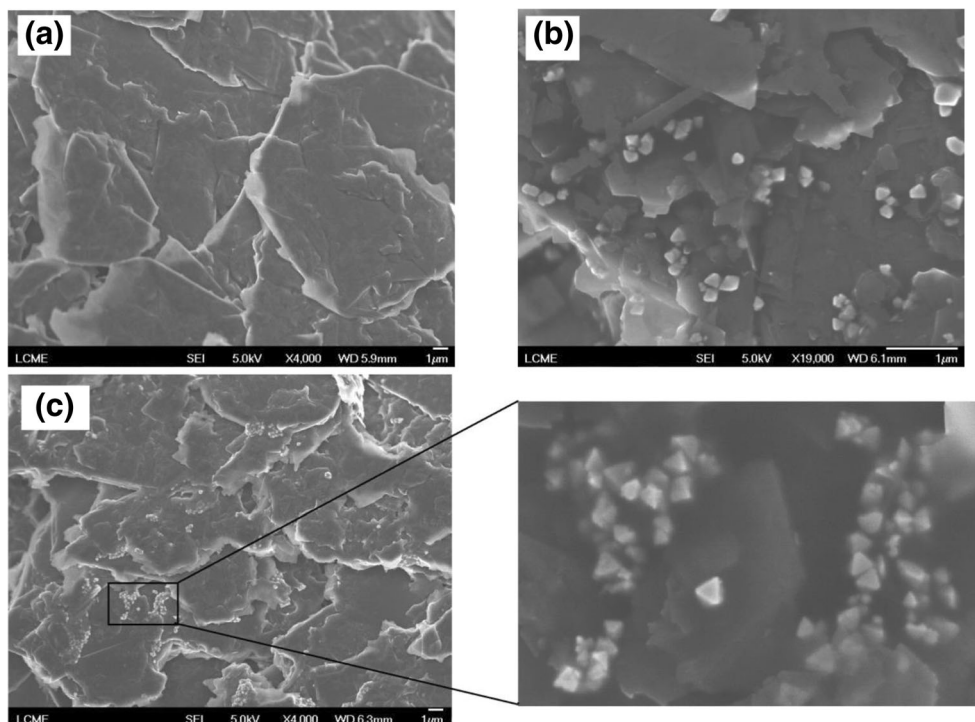
Results and discussion

Morphological and electrochemical characterization of CPE/Fe₃O₄ NP-BMI.PF₆

The morphology of the unmodified and modified electrodes in different steps of the sensor construction was evaluated by SEM-FEG. Figure 2 shows typical images for the surface of CPEs, consisting clearly distinguishable irregular carbon flakes. A clear difference in terms of surface morphology is observed between the bare CPE (Fig. 2a) and the CPE modified with Fe₃O₄ NP (Fig. 2b). The presence of Fe₃O₄ NP distributed on the graphite surface is evident. On the CPE/Fe₃O₄ NP-BMI.PF₆ surface (Fig. 2c) and in a magnified region of Fig. 2c, it can be observed that the Fe₃O₄ NP are dispersed over the electrode surface, but some agglomerates were formed, thus demonstrating the interaction of Fe₃O₄ NP with IL BMI.PF₆. In the modified CPE, the IL BMI.PF₆ acts not only as a binder for the GP but also as a bridge and as an ion carrier between the carbon layers, facilitating the electron transfer, leading to better electrode performance [1, 2, 6, 9].

The electrochemical characterization of the proposed modified electrode was performed by CV and EIS. Figure 3a shows the cyclic voltammograms obtained using the CPE/Fe₃O₄ NP-BMI.PF₆ in 0.5 mol L⁻¹ KCl solution containing 1.0 mmol L⁻¹ K₃[Fe(CN)₆] at different scan rates. As can be seen, a pair of well-defined redox peaks related to the [Fe(CN)₆]^{3-/4-} couple was obtained at the modified CPE. The insertion in Fig. 3a shows that the anodic and cathodic currents increased proportionally to the square-root of the scan rate, indicating that the electrochemical process is diffusion-controlled [40, 41]. In addition, an increase in the peak currents (about three times) and a decrease in the separation between the peak potentials (ΔE_p) of 40 mV at 50 mV s⁻¹ (data not shown) were observed for CPE/Fe₃O₄ NP-BMI.PF₆ in comparison to the unmodified CPE, indicating that the surface area increased and that the electron transfer reaction was kinetically and thermodynamically favored at the modified electrode surface. Taking into consideration that the electrochemical behavior of the [Fe(CN)₆]^{3-/4-} couple at the proposed modified electrode is very similar to that observed at traditional electrodes as platinum and glassy carbon, we concluded that the CPE/Fe₃O₄ NP-BMI.PF₆ is an electrochemical device able to

Fig. 2 SEM-FEG micrographs for **a** unmodified CPE, **b** CPE/ Fe_3O_4 NP, and **c** CPE/ Fe_3O_4 NP-BMI.PF₆ with magnification (7.5 times) of the highlighted area



detect electrochemically active ions and/or molecules and is suitable for application in electroanalyses.

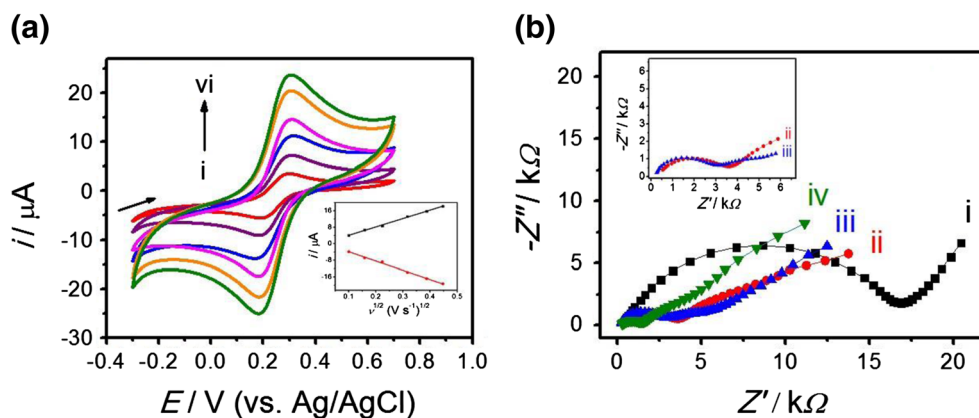
The electrodes were further characterized by EIS to obtain information on the charge transfer resistance (R_{ct}) associated with the oxidation-reduction reaction of $[\text{Fe}(\text{CN})_6]^{3-/4-}$ at the different electrodes. The Nyquist plots ($-Z''$ vs. Z') corresponding to the different electrodes are shown in Fig. 3b. The data represent the average of three experiments ($n = 3$). The R_{ct} decreased by approximately a factor of five, from 15.24 (± 0.41) $\text{k}\Omega$ with the unmodified CPE (Fig. 3b(i)) to 2.90 (± 0.04) $\text{k}\Omega$ with the CPE/ Fe_3O_4 NP (Fig. 3b(ii)). A similar behavior can be observed in Fig. 3b(iii) for the CPE/BMI.PF₆, which provided an R_{ct} of 2.62 (± 0.04) $\text{k}\Omega$ due to the presence of the IL. The lowest R_{ct} was observed with the CPE/ Fe_3O_4 NP-BMI.PF₆: 0.96 (± 0.02) $\text{k}\Omega$ (Fig. 3b(iv)). The decrease in R_{ct} can be attributed to the excellent conductive properties of the IL BMI.PF₆, which increased the

electron transfer rate between the electrode and the $[\text{Fe}(\text{CN})_6]^{3-/4-}$ probe. These experiments demonstrated the successful preparation of the chemically modified CPE with Fe_3O_4 NP and IL BMI.PF₆, which can be used as a detector for electrochemical reactions.

Electrochemical behavior of E1 at CPE/ Fe_3O_4 NP-BMI.PF₆

As shown in Fig. 4, the electrochemical response of E1 at different electrodes was investigated using CV. As expected, no peaks were observed in the absence of E1 (Fig. 4-i) at the CPE/ Fe_3O_4 NP-BMI.PF₆. After addition of 0.4 mmol L^{-1} E1 to the B-R buffer (pH 12.0), a single oxidation peak was observed at all electrodes tested in the potential window of +0.1 to +0.8 V. This indicates that the oxidation reaction of E1 is an irreversible

Fig. 3 **a** Cyclic voltammograms for 1.0 mmol L^{-1} $\text{K}_3[\text{Fe}(\text{CN})_6]$ in 0.5 mol L^{-1} KCl solution at the CPE/ Fe_3O_4 NP-BMI.PF₆ (v ($i-v$)) = 10–200 mV s^{-1}). Insertion: plot i vs. $v^{1/2}$. **b** Electrochemical impedance spectra ($n = 3$) for 5.0 mmol L^{-1} $\text{K}_3[\text{Fe}(\text{CN})_6]$ / $\text{K}_4[\text{Fe}(\text{CN})_6]$ (1:1) in 0.5 mol L^{-1} KCl solution at (i) unmodified CPE, (ii) CPE/ Fe_3O_4 NP, (iii) CPE/BMI.PF₆, and (iv) CPE/ Fe_3O_4 NP-BMI.PF₆. Insertion: curves (ii) and (iii) expanded



process, which is in agreement with previous reports [38, 42–44]. This oxidation reaction took place on the bare CPE surface (Fig. 4(ii)) at +0.430 V with an anodic current of 0.238 μA . For the modified electrodes, the oxidation peak and current were, respectively, +0.385 V and 0.882 μA for the CPE/ Fe_3O_4 NP (Fig. 4(iii)), +0.380 V and 0.919 μA for the CPE/BMI.PF₆ (Fig. 4(iv)), and +0.365 V and 1.243 μA for the CPE/ Fe_3O_4 NP-BMI.PF₆ (Fig. 4(v)). Hence, the current for the E1 oxidation was five times higher at the modified electrode compared to the unmodified CPE. The increase in the anodic current is associated with the higher surface area of the modified electrode and good conductivity provided by IL BMI.PF₆. Furthermore, the peak potential for the CPE/ Fe_3O_4 NP-BMI.PF₆ shifted 65 mV to less positive potentials compared to the unmodified CPE, demonstrating that the oxidation reaction of E1 is favored at the modified electrode. These experiments demonstrated that the use of Fe_3O_4 NP and the IL BMI.PF₆ effectively improved the properties of the CPE, increasing the electrode sensitivity and favoring the thermodynamic aspects of the estrone's reaction. However, despite the voltammetric profile suggests a pure diffusive control, it was observed that the anodic currents decreased significantly with the number of voltammetric cycles. This occurred due to the loss of available surface sites caused by adsorption (or slow desorption) of the reaction intermediates or reaction products (see discussion below), which prevent new molecules to reach the electrode surface [44, 45]. Therefore, measurements of the first cycle were used for the E1 analysis in the further experiments.

Effect of chemical composition of supporting electrolyte and solution pH

The influence of the chemical composition of the supporting electrolyte on the cyclic voltammograms of E1 was evaluated (data not shown). Initially, the supporting electrolyte was 0.2 mol L⁻¹ B–R solution. At pH values lower than 7.0, no

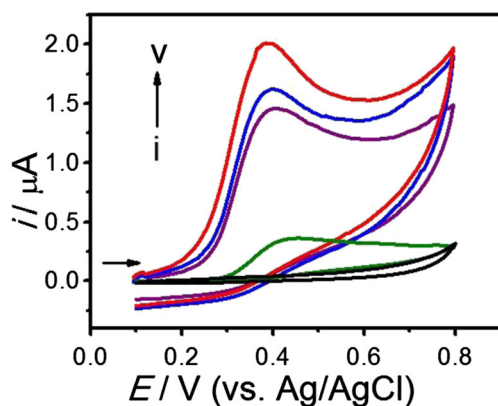


Fig. 4 Cyclic voltammograms in the (i) absence of estrone at CPE/ Fe_3O_4 NP-BMI.PF₆ (blank) and in the presence of 0.4 mmol L⁻¹ E1 in 0.2 mol L⁻¹ B–R buffer (pH 12.0) at (ii) unmodified CPE, (iii) CPE/ Fe_3O_4 NP, (iv) CPE/BMI.PF₆, and (v) CPE/ Fe_3O_4 NP-BMI.PF₆, $\nu = 50 \text{ mV s}^{-1}$

redox signal was observed. The cyclic voltammograms with the best profile were obtained at alkaline pH, as previously reported for E1 and other estrogens with similar chemical structures [44, 46, 47]. The peak current reached a maximum value in pH 12.0. Based on this information, pH 12.0 was selected to investigate the influence of the chemical composition of the different electrolytes on the electrochemical response of E1. The electrolytes tested were B–R and Ringer's buffers and NaOH solution, all at initial concentration of 0.2 mol L⁻¹. The highest peak current was obtained in B–R buffer. Therefore, this buffer solution was chosen for the subsequent analytical experiments.

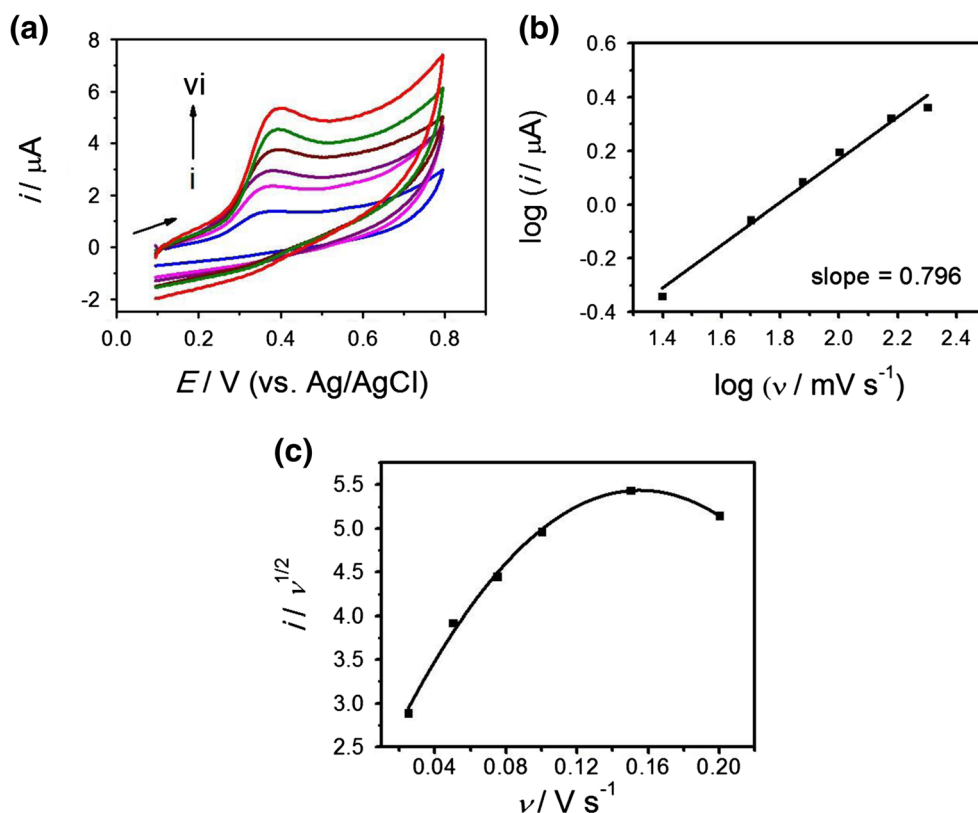
Before, the effect of the solution pH on the electrochemical behavior of E1 was also analyzed by cyclic voltammetry. The solution pH was modified between 2.0 and 12.0. It was observed that the oxidation peak potential (E_{po}) shifted linearly to less positive potentials, obeying the following equation: $E_{\text{po}}/\text{V} = (0.97 \pm 0.02) - (0.052 \pm 0.003) \text{pH}$ ($r = 0.993$). The slope of the straight line obtained was -52 mV pH^{-1} . For pH-dependent reversible reactions, the slope of $E_{\text{p}} \times \text{pH}$ plot is -59 mV pH^{-1} , according to the Nernst equation, indicating that equal number of electrons and protons participate in the reaction [42, 44]. Although the electrochemical oxidation reaction of E1 is irreversible, as shown above, the slope of the graph $E_{\text{po}} \times \text{pH}$ suggests that the reaction path may be like that of a reversible reaction. We will consider this observation in the discussion of the E1 oxidation mechanism (see below).

Influence of scan rate

Cyclic voltammograms were obtained at different scan rates between 25 and 200 mV s^{-1} for 0.4 mmol L⁻¹ E1 in 0.2 mol L⁻¹ B–R buffer (pH 12.0) at the CPE/ Fe_3O_4 NP-BMI.PF₆. The curves obtained are shown in Fig. 5a. The oxidation peak currents increased linearly with the scan rate. The slope of $\log i$ vs. $\log \nu$ (Fig. 5b) was 0.796. According to the literature, a slope equal of (or close to) 1.0 indicates that the reaction is controlled by adsorption [48]. Therefore, we can conclude that the E1 oxidation reaction on CPE is an adsorption-controlled process, obeying the following equation: $\log i = (0.80 \pm 0.04) \log \nu - (1.42 \pm 0.09)$. This behavior is similar to that reported in the literature [38, 43, 44, 49]. In addition, the data agree with those discussed earlier, which demonstrated that the anodic current decreases with the increasing number of voltammetric cycles, suggesting adsorption of products. Furthermore, the interdependence between the current function ($i \nu^{-1/2}$) and ν (Fig. 5c) indicates the presence of chemical reactions coupled to the oxidation reaction of E1.

The data collected on the influence of the solution pH and the potential scan rate on the electrochemical behavior of E1 at the CPE/ Fe_3O_4 NP-BMI.PF₆ allow some speculations regarding its oxidation mechanism. The mechanism for the

Fig. 5 **a** Cyclic voltammograms for 0.4 mmol L⁻¹ E1 in 0.2 mol L⁻¹ B–R buffer (pH 12.0) at CPE/Fe₃O₄ NP-BMI.PF₆, ν ($i-v$) = 25–200 mV s⁻¹. **b** Plot $\log i$ vs. $\log \nu$. **c** Plot $i \nu^{-1/2}$ vs. ν



electrochemical oxidation of E1 seems to follow the typical oxidation of phenolic compounds having just one hydroxyl group in their structure. Hence, we propose that the electrochemical oxidation of E1 mainly produces quinone via an irreversible electrochemical reaction involving the transfer of 2 mol of protons and 2 mol of electrons, in agreement with other authors [44, 45, 47]. Figure 6 below shows the proposed reaction for E1 oxidation at the CPE/Fe₃O₄ NP-BMI.PF₆. However, the $i \nu^{-1/2}$ vs. ν plot indicates the presence of coupled chemical reaction(s) after the electrochemical step. Hence, an EC mechanism [50] could be observed, where E is the electrochemical step (at the electrode) and C the chemical step in solution. The resulting products depend on the rearrangements in the oxidized molecule.

Accumulation potential and time

The influence of accumulation potential (E_{acc}) and accumulation time (t_{acc}) on the oxidation peak current of 0.4 mmol L⁻¹ E1 was investigated in 0.2 mol L⁻¹ B–R buffer (pH 12.0) (data not shown). Initially, the E_{acc} was varied in the range of –0.4

to +0.3 V at constant t_{acc} of 5 s. The E_{acc} selected was –0.4 V because it provided the highest oxidation peak current. In the next step, the t_{acc} was varied between 0 and 25 s at constant $E_{acc} = -0.4$ V. The optimized value was 5 s. For t_{acc} higher than 5 s, a decrease in the oxidation peak current of E1 was observed, suggesting a saturation of the modified electrode surface. Other researchers have reported a similar behavior [38, 43, 49]. In conclusion, $E_{acc} = -0.4$ V and $t_{acc} = 5$ s were selected for subsequent experiments.

Calibration curve

Different electroanalytical techniques were investigated to evaluate the sensitivity of the CPE/Fe₃O₄ NP-BMI.PF₆ for E1 detection: linear scan voltammetry (LSV), differential-pulse voltammetry (DPV), and square-wave voltammetry (SWV). The SWV technique showed higher sensitivity, better peak definition, and lower potential for E1 oxidation. Hence, SWV was chosen for subsequent experiments. The parameters of SWV scan increment (ΔE_s), amplitude (a), and frequency (f) were optimized by Box–Behnken factorial design

Fig. 6 Proposed reaction for estrone oxidation at the CPE/Fe₃O₄ NP-BMI.PF₆

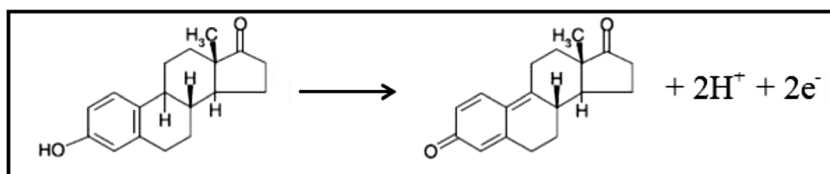


(Table S2; Fig. S2). The maximum response of current was reached using $\Delta E_s = 2.8$ mV, $a = 90$ mV, and $f = 30$ Hz.

Applying the optimized experimental conditions, the calibration curve ($n = 8$) was obtained by successive additions of a standard solution of E1. The voltammograms revealed a well-defined oxidation peak at +0.308 V. The peak current increased with increasing E1 concentration (Fig. 7a). The calibration curve (Fig. 7b) displays two ranges of linearity: the first (I) between 4.0 and 9.0 $\mu\text{mol L}^{-1}$: $i/\mu\text{A} = (0.237 \pm 0.007) [\text{E1}] / \mu\text{mol L}^{-1} - (0.61 \pm 0.04)$, $r = 0.998$ and the second (II) between 9.0 and 100.0 $\mu\text{mol L}^{-1}$: $i/\mu\text{A} = (0.0458 \pm 0.0010) [\text{E1}] / \mu\text{mol L}^{-1} + (1.10 \pm 0.04)$, $r = 0.998$. The two linear ranges with distinct slopes may be related to the saturation of the electrode surface. According to the increase in the E1 concentration, the interaction of the molecules with the modified surface of the electrode decreases, which explains the drop in the sensitivity, in agreement with the findings presented by other authors [51]. The limit of detection (LOD) was calculated according to equation: $\text{LOD} = 3 \text{ Sb} / B$, where Sb is the standard deviation of the linear coefficient (0.037 μA) and B is the slope of the calibration curve (0.237 $\mu\text{A L} \mu\text{mol}^{-1}$). The limit of quantification (LOQ) was determined using the visual method [52]. The LOD and LOQ values obtained were 0.47 and 4.0 $\mu\text{mol L}^{-1}$, respectively. For comparison purposes, a calibration curve was also constructed using an unmodified CPE under the same experimental conditions (Fig. S3). The LOD and LOQ values obtained with the CPE were 12.89 and 42.97 $\mu\text{mol L}^{-1}$, respectively. These results indicate that the CPE/ Fe_3O_4 NP-BMI.PF₆ is more sensitive than the unmodified CPE in relation to E1 detection. The repeatability of the current provided by the CPE/ Fe_3O_4 NP-BMI.PF₆ was tested by means of two methods: intra-day, using eight different solutions prepared on the same day at concentrations of 9.0, 60.0, and 100.0 $\mu\text{mol L}^{-1}$, and inter-day, over 8 days using different solutions of E1 prepared each day at concentrations of 9.0, 60.0, and 100.0 $\mu\text{mol L}^{-1}$. The relative standard deviations (RSD) for measurements of the anodic current carried out in intra- and inter-day studies were lower than 3.5%, indicating the excellent repeatability furnished by the CPE/ Fe_3O_4 NP-BMI.PF₆, which can be used as a sensor for determining the E1 concentration.

Comparison with other techniques and modified electrodes

The performance of the CPE/ Fe_3O_4 NP-BMI.PF₆ using SWV for the determination of E1 was compared to that of other techniques and modified electrodes described in the literature (Table 1). It is not surprising that the proposed modified electrode associated to the SWV showed a linear range for higher E1 concentrations and, consequently, a higher LOD than chromatographic techniques [34, 35]. On the other hand, it exhibited a linear range and a LOD similar to those of CE [37]. Owing to concern the use of electroanalytical techniques and modified electrodes, Jin and collaborators [42] used a carbamylcholine-modified paraffin-impregnated graphite electrode. The linear range was between 0.3 and 30.0 $\mu\text{mol L}^{-1}$ and the LOD was 0.1 $\mu\text{mol L}^{-1}$. Lin and coworkers [49] employed a Pt nano-clusters/multi-walled carbon nanotubes-modified glassy carbon electrode and reported a linear range of 2.0 to 50.0 $\mu\text{mol L}^{-1}$ and a LOD of 0.84 $\mu\text{mol L}^{-1}$. Using a glassy carbon electrode modified with multi-walled carbon nanotubes functionalized with congo red, the authors [38] obtained a linear range of 0.05 to 20.0 $\mu\text{mol L}^{-1}$ and a LOD of 0.005 $\mu\text{mol L}^{-1}$. As can be seen, the LOD obtained with the proposed electrode (0.47 $\mu\text{mol L}^{-1}$) is not the lowest, but the calibration curve (4.0 to 100.0 $\mu\text{mol L}^{-1}$) is the most extensive. Moreover, the CPE/ Fe_3O_4 NP-BMI.PF₆ is easy to prepare and cheaper. Finally, as it will be described in the next section, the proposed modified electrode was able to detect E1 in a complex sample such as pork meat.

Application of the CPE/ Fe_3O_4 NP-BMI.PF₆ for determination of E1 in pork meat samples and comparative studies

The SWV data obtained with the proposed CPE/ Fe_3O_4 NPs-BMI.PF₆ for the determination of E1 in three simulated pork meat samples were compared with the data provided by the UV-vis technique. Table 2 summarizes the results obtained

Fig. 7 **a** Square-wave voltammograms for the (i) blank and different concentrations of estrone (ii–xvi) (4.0–100.0 $\mu\text{mol L}^{-1}$) in 0.2 mol L^{-1} B–R buffer solution (pH 12.0) at the CPE/ Fe_3O_4 NP-BMI.PF₆, $E_{\text{acc}} = -0.4$ V; $t_{\text{acc}} = 5$ s; $\Delta E_s = 2.8$ mV, $a = 90$ mV, and $f = 30$ Hz. **b** Calibration curve for estrone ($n = 8$) at CPE/ Fe_3O_4 NP-BMI.PF₆

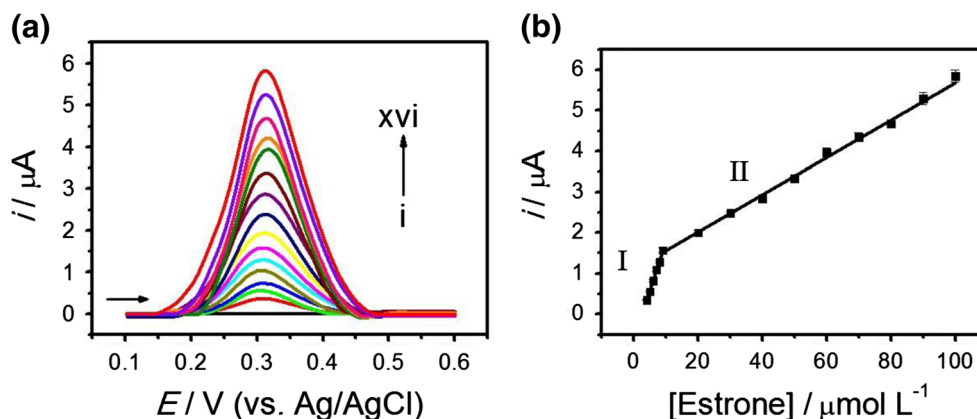


Table 1 Comparison with previously reported technique and electrodes

Technique	Analyzed sample	Linear range ($\mu\text{mol L}^{-1}$)	LOD ($\mu\text{mol L}^{-1}$)	Reference
SPE-HPLC-MS ^a	Milk	0.0011–0.055	0.0003	[34]
SPME-HPLC ^b	Milk and urine	0.002–0.055	0.0012	[35]
CE ^c	Human urine	0.37–55.48	0.11	[37]
SWV ^d	Blood serum	0.3–30.0	0.10	[42]
SWV ^e	Blood serum	2.0–50.0	0.84	[49]
LSV ^f	Tablets	0.05–20.0	0.005	[38]
SWV ^g	Pork meat	9.0–100.0 ^h	0.47	This work

^a Solid-phase extraction coupled with high-performance liquid chromatography-mass spectrometry

^b Solid-phase microextraction coupled with high-performance liquid chromatography

^c Capillary electrophoresis

^d Square-wave voltammetry with carbamylcholine-modified paraffin-impregnated graphite electrode

^e Square-wave voltammetry with Pt nano-clusters/multi-walled carbon nanotubes-modified glassy carbon electrode

^f Linear sweep voltammetry with glassy carbon electrode modified with multi-walled carbon nanotubes functionalized with congo red

^g Square-wave voltammetry with carbon paste electrode modified with Fe₃O₄ NP and IL BMI.PF₆

^h Wider range

and the statistical analysis of data. As no trace of E1 was detected in preliminarily analyzed pork meat samples, they were fortified with the hormone. Ethanolic extracts of E1 were prepared at concentrations of 70.0, 80.0, and 90.0 $\mu\text{mol L}^{-1}$. The analytical studies were carried out using the second linear range because it permits the analysis of a wide E1 concentration range. Square-wave voltammograms were recorded in the range of +0.1 to +0.6 V. The electro-analytical determinations of E1 were carried out using the method of external calibration. As can be seen in Table 2, the E1 contents determined by both techniques were very close to the values accepted as true. The relative standard deviation (RSD) for the mean of eight determinations of E1 in the three samples was between 3.92 and 4.52% for the measurements with CPE/Fe₃O₄ NP-BMI.PF₆ and between 3.13 and 4.40% using the UV–vis technique. In addition, the statistical treatment applied to the results obtained

clearly demonstrates the reliability of the data provided by the two techniques. Two of the most widely used tests for the comparison of results are the *t* and *F* tests. The *t* test was used to compare the results obtained by the two techniques with the true values. At the 95% confidence level, all values calculated for *t*_{value} were lower than that for *t*_{critical} (2.360), indicating no significant differences between the data obtained using the two techniques and the true values. The discrepancy between the data provided by CPE/Fe₃O₄ NP-BMI.PF₆ and UV–vis techniques was verified by applying the *F* test. The values for *F* value obtained in the determination of E1 in pork meat samples were lower than that for *F*_{critical} (3.787) at the 95% confidence level, indicating that there is no significant difference in the precision provided by the two techniques. Thus, it can be concluded that the CPE/Fe₃O₄ NP-BMI.PF₆ is an excellent sensor for E1 detection in pork meat.

Table 2 Determination of E1 in pork meat samples

Sample	A		B		C	
	UV–vis	SWV	UV–vis	SWV	UV–vis	SWV
Added values ($\mu\text{mol L}^{-1}$)	70.0	70.0	80.0	80.0	90.0	90.0
Found values ($\mu\text{mol L}^{-1}$) ^a	68.871	68.497	78.633	77.510	88.691	88.167
RSD (%)	4.396	4.525	3.127	4.536	3.336	3.924
<i>E</i> _r (%) ^b	–0.543		–1.428		–0.591	
<i>t</i> _{value} ^c	0.341	0.341	0.903	0.903	0.428	0.428
<i>F</i> _{value} ^d	1.048		2.044		1.368	

^a *n* = 8

^b *E*_r = relative error between SWV with the proposed CPE/Fe₃O₄ NP-BMI.PF₆ and UV–vis

^c *t*_{critical} = 2.360

^d *F*_{critical} = 3.787

Interference of matrix components

As a final point, the interference of matrix components on the analytical signal (current from E1 oxidation) was examined by comparing the slopes of the calibration curve and of a standard addition curve built for this purpose. This procedure is advantageous comparing to traditional interference studies because evaluates the disturbance (or not) of all constituents of matrix, at real concentration, on the analytical response provided by E1 oxidation. The traditional study of interferents is time consuming and, in most cases, evaluates potential interferents that are not present in the sample matrix. The slopes of the two curves were similar. The slope of the calibration curve was of $0.046 \mu\text{A L } \mu\text{mol}^{-1}$, while that of the standard addition curve was $0.047 \mu\text{A L } \mu\text{mol}^{-1}$. This signifies that the components of pork meat samples do not interfere in the determination of E1. Hence, another remarkable property of the CPE can be noticed: it was able to detect E1 selectively in the presence of the other components present in the pork meat samples.

Conclusions

A simple, rapid, and sensitive chemically modified electrode was successfully employed for the voltammetric determination of E1, based on Fe_3O_4 NP and IL BMI.PF₆. Due to the combination of the electrocatalytic properties of the NP and high conductivity of IL, the proposed modified electrode improved the oxidation of E1, increasing its oxidation peak current and lowering its oxidation potential. The catalytic effect promoted by Fe_3O_4 NP could be interpreted as follows: its presence at the CPE increased the surface area, which allowed the increase of E1 diffusion to the modified electrode and in the frequency of contact of the E1 molecules with the electrode surface, increasing the reaction rate-determining step and shifting the oxidation potential to less positive values. The modified electrode was successfully applied in the determination of E1 in complex matrices such as in pork meat samples. The results were comparable to those obtained by UV–vis technique. Moreover, the statistical treatments demonstrated the precision and accuracy of the data provided by the new modified electrode. Hence, the outstanding performance of the proposed CPE indicates that Fe_3O_4 NP and IL BMI.PF₆ are promising materials for the construction and application of new chemically modified electrodes for the determination of E1 or other estrogens with similar chemical structure.

Acknowledgements The authors are grateful to the Brazilian government agencies CNPq (Conselho Nacional de Desenvolvimento Científico e Tecnológico), CAPES (Coordenação de Aperfeiçoamento de Pessoal de Nível Superior), and FAPESC (Fundação de Amparo à Pesquisa e Inovação do Estado de Santa Catarina) for the scholarship and financial support. We are also in debt with Central Laboratory of Electron Microscopy of Federal University of Santa Catarina (Florianópolis/SC,

Brazil) due to the surface analyses and with LacBio (Laboratório de Catálise Biomimética) for providing the IL BMI.PF₆.

References

- Daneshvar L, Rounaghi G, E'shaghi Z, Chamsaz M, Tarahomi S (2016) Electrochemical determination of carbamazepin in the presence of paracetamol using a carbon ionic liquid paste electrode modified with a three-dimensional graphene/MWCNT hybrid composite film. *J Mol Liq* 215:316–322
- Taei M, Salavati H, Hasanpour F, Habibollahi S, Baghlani H (2016) Simultaneous determination of ascorbic acid, acetaminophen and codeine based on multi-walled carbon nanotubes modified with magnetic nanoparticles paste electrode. *Mater Sci Eng C* 69:1–11
- Ensafi AA, Abarghoui MM, Rezaei B (2015) Simultaneous determination of morphine and codeine using Pt nanoparticles supported on porous silicon flour modified ionic liquid carbon paste electrode. *Sens Actuators B: Chem* 219:1–9
- Li Y, Zhai X, Liu X, Wang L, Liu H, Wang H (2016) Electrochemical determination of bisphenol A at ordered mesoporous carbon modified nano-carbon ionic liquid paste electrode. *Talanta* 148:362–369
- Mani V, Wu TY, Chen SM (2014) Iron nanoparticles decorated graphene-multiwalled carbon nanotubes nanocomposite-modified glassy carbon electrode for the sensitive determination of nitrite. *J Solid State Electrochem* 18:1015–1023
- Heli H, Majidi S, Sattarahmady N, Parsaei A (2010) Electrocatalytic oxidation and sensitive detection of deferoxamine on nanoparticles of $\text{Fe}_2\text{O}_3@ \text{NaCo}[\text{Fe}(\text{CN})_6]$ -modified paste electrode. *J Solid State Electrochem* 14:1637–1647
- Yang S, Li G, Wang G, Deng D, Qu L (2015) A novel electrochemical sensor based on Fe_2O_3 nanoparticles/N-doped graphene for electrocatalytic oxidation of L-cysteine. *J Solid State Electrochem* 9:3613–3620
- Gholivand MB, Torkashvand M, Yavari E (2015) Electrooxidation behavior of warfarin in Fe_3O_4 nanoparticles modified carbon paste electrode and its determination in real samples. *Mater Sci Eng C* 48: 235–242
- Yu C, Lo N, Cheng H, Tsuda T, Sakamoto T, Chen Y, Kuwabata S, Chen P (2014) An ionic liquid- Fe_3O_4 nanoparticles-graphite composite electrode used for nonenzymatic electrochemical determination of hydrogen peroxide. *J Electroanal Chem* 729:109–115
- Benvidi A, Jahanbani S (2016) Self-assembled monolayer of SH-DNA strand on a magnetic bar carbon paste electrode modified with $\text{Fe}_3\text{O}_4@ \text{Ag}$ nanoparticles for detection of breast cancer mutation. *J Electroanal Chem* 768:47–54
- Silveira JP, Piovesan JV, Spinelli A (2017) Carbon paste electrode modified with ferrimagnetic nanoparticles for voltammetric detection of the hormone estriol. *Microchem J* 133:22–30
- Hu Y, Zhang Z, Zhang H, Luo L, Yao S (2012) Selective and sensitive molecularly imprinted sol–gel film-based electrochemical sensor combining mercaptoacetic acid-modified PbS nanoparticles with $\text{Fe}_3\text{O}_4@ \text{Au}$ -multi-walled carbon nanotubes–chitosan. *J Solid State Electrochem* 16:857–867
- Kingsley MP, Desai PB, Srivastava AK (2015) Simultaneous electro-catalytic oxidative determination of ascorbic acid and folic acid using Fe_3O_4 nanoparticles modified carbon paste electrode. *J Electroanal Chem* 741:71–79
- Parsaei M, Asadi Z, Khodadoust S (2015) A sensitive electrochemical sensor for rapid and selective determination of nitrite ion in water samples using modified carbon paste electrode with a newly synthesized cobalt(II)-Schiff base complex and magnetite nanospheres. *Sens Actuators B: Chem* 220:1131–1138

15. Mohammadi N, Najafi M, Adeg NB (2017) Highly defective mesoporous carbon-ionic liquid paste electrode as sensitive voltammetric sensor for determination of chlorogenic acid in herbal extracts. *Sens Actuators B: Chem* 243:838–846
16. Arvand M, Hassannezhad M (2014) Magnetic core-shell $\text{Fe}_3\text{O}_4@/\text{SiO}_2/\text{MWCNT}$ nanocomposite modified carbon paste electrode for amplified electrochemical sensing of uric acid. *Mater Sci Eng C* 36:160–167
17. Al-Zahrani E, Soomro MT, Bashami RM, Rehman AU, Danish E, Ismail IMI, Aslam M, Hameed A (2016) Fabrication and performance of magnetite (Fe_3O_4) modified carbon paste electrode for the electrochemical detection of chlorite ions in aqueous medium. *J Environ Chem Eng* 4:4330–4341
18. Gerent GG, Spinelli A (2017) Magnetite-platinum nanoparticles-modified glassy carbon electrode as electrochemical detector for nitrophenol isomers. *J Hazard Mater* 330:105–115
19. Baezzat MR, Banavand F, Fasihi F (2017) Electrooxidation study and highly sensitive voltammetric determination of alfuzosin employing multi-walled carbon nanotubes and the ionic liquid 1-hexylpyridinium hexafluorophosphate nanocomposite sensor. *J Mol Liq* 233:391–397
20. Siddiquee S, Yusof NA, Salleh AB, Tan SG, Bakar FA (2012) Development of electrochemical DNA biosensor for *Trichoderma harzianum* based on ionic liquid/ ZnO nanoparticles/chitosan/gold electrode. *J Solid State Electrochem* 16:273–282
21. Casado-Carmona FA, Alcludia-León MC, Lucena R, Cárdenas S, Valcárcel M (2016) Magnetic nanoparticles coated with ionic liquid for the extraction of endocrine disrupting compounds from waters. *Microchem J* 128:347–353
22. Chen Y, Huang Y, Guo D, Chen C, Wang Q, Fu Y (2014) A chiral sensor for recognition of DOPA enantiomers based on immobilization of β -cyclodextrin onto the carbon nanotube-ionic liquid nanocomposite. *J Solid State Electrochem* 18:3463–3469
23. Babu RS, Prabhu P, Narayanan SS (2016) Facile immobilization of potassium-copper hexacyanoferrate nanoparticles using a room-temperature ionic liquid as an ionic binder and its application towards BHA determination. *J Solid State Electrochem* 20:1575–1583
24. Monerri MJ, D'Eramo F, Arévalo FJ, Fernández H, Zon MA, Molina PG (2016) Electrochemical immunosensor based on gold nanoparticles deposited on a conductive polymer to determine estrone in water samples. *Microchem J* 129: 71–77
25. Lahcen AA, Baleb AA, Baker P, Iwuoha E, Amine A (2017) Synthesis and electrochemical characterization of nanostructured magnetic molecularly imprinted polymers for 17- β -estradiol determination. *Sens Actuators B: Chem* 241:698–705
26. Fonseca AP, Lima DLD, Esteves VI (2011) Degradation by solar radiation of estrogenic hormones monitored by UV-visible spectroscopy and capillary electrophoresis. *Water Air Soil Pollut* 215: 441–447
27. Perez C, Simões FR, Codognoto L (2015) Voltammetric determination of 17 α -ethinylestradiol hormone in supply dam using BDD electrode. *J Solid State Electrochem* 20:2471–2478
28. Ji L, Wang Y, Wu K, Zhang W (2016) Simultaneous determination of environmental estrogens: diethylstilbestrol and estradiol using Cu-BTC frameworks-sensitized electrode. *Talanta* 159:215–221
29. Goh SXL, Duarac A, Zhang L, Snyder SA, Lee HK (2016) Online solid phase extraction with liquid chromatography-tandem mass spectrometry for determination of estrogens and glucocorticoids in water. *J Chromatogr A* 1465:9–19
30. Vanhaecke L, Bussche JV, Wille K, Bekaert K, Brabander HF (2011) Ultra-high performance liquid chromatography-tandem mass spectrometry in high-throughput confirmation and quantification of 34 anabolic steroids in bovine muscle. *Anal Chim Acta* 700: 70–77
31. Xu X, Liang F, Shi J, Zhao X, Liu Z, Wu L, Song Y, Zhang H, Wang Z (2013) Determination of hormones in milk by hollow fiber-based stirring extraction bar liquid-liquid microextraction gas chromatography mass spectrometry. *Anal Chim Acta* 790:39–46
32. Wang J, Chen Z, Li Z, Yang Y (2016) Magnetic nanoparticles based dispersive micro-solid-phase extraction as a novel technique for the determination of estrogens in pork samples. *Food Chem* 204:135–140
33. Sales RL, Rocha JLM, Bressan J (2015) Utilização de hormônios e antibióticos em produtos alimentícios de origem animal: aspectos gerais e toxicológicos. *Nutrire* 40:409–420
34. Yan W, Li Y, Zhao L, Lin J (2009) Determination of estrogens and bisphenol A in bovine milk by automated on-line C_{30} solid-phase extraction coupled with high-performance liquid chromatography-mass spectrometry. *J Chromatogr A* 1216:7539–7545
35. Hu Y, Fan Y, Li G (2012) Preparation and evaluation of a porous monolithic capillary column for microextraction of estrogens from urine and milk samples online coupled to high-performance liquid chromatography. *J Chromatogr A* 1228:205–212
36. Albero B, Sánchez-Brunete C, Miguel E, Tadeo JL (2017) Application of matrix solid-phase dispersion followed by GC-MS/MS to the analysis of emerging contaminants in vegetables. *Food Chem* 217:660–667
37. Flor S, Lucangioli S, Contin M, Tripodi V (2010) Simultaneous determination of nine endogenous steroids in human urine by polymeric-mixed micelle capillary electrophoresis. *Electrophoresis* 31:3305–3313
38. Yang C, Sang Q, Zhang S, Huang W (2009) Voltammetric determination of estrone based on the enhancement effect of surfactant and a MWNT film electrode. *Mater Sci Eng C* 29: 1741–1745
39. Sun W, Chen XQY, Liu S, Gao H (2011) Application of chitosan/ Fe_3O_4 microsphere-graphene composite modified carbon ionic liquid electrode for the electrochemical detection of the PCR product of soybean lectin gene sequence. *Talanta* 87:106–112
40. Nicholson RS, Shain I (1964) Theory of stationary electrode polarography single scan and cyclic methods applied to reversible, irreversible, and kinetic systems. *Anal Chem* 36:706–723
41. Bard AJ, Faulkner L (2001) *Electrochemical methods, fundamentals and applications*. Wiley, New York
42. Jin G, Lin X (2005) Voltammetric behavior and determination of estrogens at carbamylcholine modified paraffin-impregnated graphite electrode. *Electrochim Acta* 50:3556–3562
43. Luo L, Li F, Zhu L, Ding Y, Deng D (2013) Electrochemical sensing platform of natural estrogens based on the poly(L-proline)-ordered mesoporous carbon composite modified glassy carbon electrode. *Sens Actuators B: Chem* 187:78–83
44. Brocenschi RF, Rocha-Filho RC, Li L, Swain GM (2014) Comparative electrochemical response of estrone at glassy-carbon, nitrogen-containing tetrahedral amorphous carbon and boron-doped diamond thin-film electrodes. *J Electroanal Chem* 712: 207–214
45. Ngundi MM, Sadik OA, Yamaguchi T, Suye S (2003) First comparative reaction mechanisms of β -estradiol and selected environmental hormones in a redox environment. *Electrochem Commun* 5:61–67
46. Vega D, Agüí L, González-Cortés A, Yáñez-Sedeño P, Pingarrón JM (2007) Electrochemical detection of phenolic estrogenic compounds at carbon nanotube-modified electrodes. *Talanta* 71: 1031–1038
47. Santos KD, Braga OC, Vieira IC, Spinelli A (2010) Electroanalytical determination of estriol hormone using a boron-doped diamond electrode. *Talanta* 80:1999–2006
48. Gosser DK (1993) *Cyclic voltammetry: simulation and analysis of reaction mechanisms*. VCH, New York

49. Lin X, Li Y (2006) A sensitive determination of estrogens with a Pt nano-clusters/multi-walled carbon nanotubes modified glassy carbon electrode. *Biosens Bioelectron* 22:253–259
50. Brett CA, Brett AMO (1993) *Electrochemistry principles, methods, and applications*. New York, Oxford
51. Silva TR, Westphal E, Gallardo H, Vieira IC (2014) Ionic organic film sensor for determination of phenolic compounds. *Electroanalysis* 26:1801–1809
52. Ribani M, Bottoli CBG, Collins CH, Jardim ICSF, Melo LFC (2004) Validação em métodos cromatográficos e eletroforéticos. *Quim Nova* 5:771–780